

PERFORMANCE OF CASCADED H-BRIDGE INVERTER INTEGRATED WITH HFT FOR PV SYSTEM APPLICATIONS

Mahrous Ahmed¹, I. Taha²

¹Aswan Faculty of Engineering, Aswan university, Aswan, Egypt

²Tanta University, Faculty of engineering, Tanta, Egypt

ABSTRACT

This paper presents a photovoltaic system as a standalone system. The proposed system consists of photovoltaic (PV) module, battery energy storage system (BESS), high frequency transformer, and multilevel inverter (MLI). The MLI consists of two H-bridge single phase inverter per arm (phase) with unequal dc voltages which needs 6 isolated dc sources for the conventional MLI. The relative values between the upper (auxiliary) inverter dc voltage and the lower H-bridge (main) inverter is 1/3 resulting in 9 levels MLI. Each isolated dc source comes from a PV module accompany with a BESS. A high frequency transformer (HFT) is proposed in this paper to generate the dc bus voltage of the auxiliary inverter from the main inverter dc bus voltage. As a result of that the number of isolated dc bus voltages required is reduced by half which is reflected in reducing the number of PV required and thus reducing the cost of the overall system. In addition, a natural balancing between the main and auxiliary inverters dc bus voltages of each arm will be attained due to the HFT turns ratio which result in simplifying the overall control of the whole system. In order to reduce the size of the HFT a judicious modulation index (MI) will be chosen. The proposed system has been simulated using static inductive load. Analyses and simulation have been proposed to validate the proposed control scheme.

يقترح هذا البحث نظام توليد طاقة كهربية باستخدام نظام طاقة شمسية كمصدر معزول ووحيد للتغذية، والنظام المقترح عبارة عن نموذج لخلية شمسية مع نظام شحن للبطاريات ومحول عالي التردد مع عاكس متعدد المستويات. يتكون العاكس متعدد المستويات من عاكسين متصلين على التوالي لكل وجه من النوع (H-bridge) ويكون جهد التغذية لهما غير متساوي، و يتطلب العاكس في الحالة العادية إلى عدد 6 مصادر جهد مستمر لتغذية العاكس ثلاثي الأطوار منفصلة بحيث يكون النسبة بين جهد العاكسين الفرعي والرئيسي هي 1/3 و هذا يؤدي بدوره إلى زيادة دقة الخرج له إلى أقصى درجة. يستخدم المحول عالي التردد لتوصيل الجهد للعاكس الفرعي من الرئيسي بالنسبة السابقة، ومن ثم فإن عدد مصادر التيار المستمر يقل للنصف ومن ثم تقل وحدات الطاقة الشمسية المطلوبة وهو ما يقلل التكلفة الكلية. من المميزات الأخرى لاستخدام المحول عالي التردد لتسهيل دائرة التحكم المطلوبة للنظام الكلي. و أيضاً لتقليل قدرة المحول عالي التردد سوف يتم اختيار القيمة المناسبة لمعامل تقطيع العاكس مما يؤدي إلى تقليل حجم المحول المطلوب. وفي النهاية سوف يتم تمثيل وتحليل النظام المقترح على حمل إستاتيكي للتحقق من جودة أداءه.

Keywords — MLI; PV; HF Transformer; bidirectional converter; Isolated dc sources.

1. Introduction

Today world is facing a cute energy shortage due to the increase of the average consumption of energy per capita. Therefore renewable energy systems are a promising application with great interest in clean and renewable energy sources. The photovoltaic system is the second important renewable energy sources after the wind power sources. Two main applications of the PV systems, grid connected and standalone systems [1] – [2]. Standalone PV power systems are electrical power systems energized by photovoltaic panels which are independent of the utility grid. In standalone photovoltaic power systems, the electrical energy produced by the photovoltaic panels cannot

always be used directly. As the demand from the load does not always equal the solar panel capacity, battery banks are generally used. The growing number of research in power electronics has decreased the initial cost of these system and facilitated their use around the world.

In recent years, there has been great interest in multilevel inverters (MLIs) technology. Special attention has been paid for cascaded H-bridge inverter [3] – [7]. Generally, there are many advantages in the applications of MLIs inverters over conventional two-level inverters. The series connection of power converter modules reduces the voltage stress of each converter module (or increases the voltage capability of the overall converter

structure). Besides, the resolution of the staircase waveform of the output voltage increases with the number of voltage steps of capacitor voltage sources available in the multilevel inverter [5]. As a result of the improved resolution in the voltage harmonic content, filtering efforts and the level of the electromagnetic interference (EM) generated by the switching operation of the converter can be reduced.

Despite this important improvement, these topologies have an important drawback: They need many isolated power supplies that must be balanced. These balanced isolated sources are generated from the PV system for the considered situation in this paper. This reason, costly and complex topologies have to be implemented to get many isolated supplies. Some solutions using cascaded multilevel inverters with a single power source and without transformers have been introduced recently [8] – [9]. However, these solutions use floating capacitors with complex balancing systems and many more semiconductors in relation to the number of levels produced.

The objective of this paper is to develop a new dc-link topology for cascaded H-bridge inverter with maximum voltage resolution, based on a simple High Frequency Link (HFL) with small size, which allows using only one power supply (battery pack, fuel cell or other) for single arm. The system has inherent regulation of the voltages supplied among the H-bridges, so the full number of levels can be produced at any amplitude of voltage, depending only on the single-dc-supply regulation per arm, which can be controlled with a chopper. This proposed topology does not need floating capacitors or heavy bulky transformers.

2. Cascaded H-Bridge Inverter Integrated with HFT

Fig. 1 represents the schematic diagram of the 3-phase 9-level 24-switch VSI. For convenience, all the switches and diodes have been considered to be ideal; moreover, voltage fluctuations of dc bus voltage also considering absent. It has two single phase H-bridge inverters modules per phase (arm). The ratio of the dc power supplies is 1/3 which enables developing the maximum output voltage resolution. The H-bridge module with lower dc voltage source is the auxiliary inverter and the H-bridge with greater dc voltage source is the main inverter. That is due to the load power contribution is mainly provided from the main inverter. In this topology, each phase is containing 2-dc sources. Which are V_{dc} and $3V_{dc}$. Therefore the maximum dc multilevel output voltage level can be produced $(V_{dc}+3V_s) = 4V_{dc}$ and the minimum output level of dc voltage can be 0V. Hence some possible options are proposed to create $(4 \times 2 + 1 = 9)$ levels in AC

voltage wave shape, if there are one volt level difference between every two congested level.

Table I shows the switching states and the load node voltage referred to the neutral of the dc bus voltage (v_{aN}) for Arm ‘a’. The load line-to-line voltages can be calculated as follows:

$$v_{ab} = v_{aN} - v_{bN} \tag{1}$$

Therefore the load line-to-line voltages can have $(9V_{dc}, 8V_{dc}, 7V_{dc}, 6V_{dc}, 5V_{dc}, 4V_{dc}, 3V_{dc}, 2V_{dc}, 1V_{dc}, 0V_{dc}, -1V_{dc}, -2V_{dc}, -3V_{dc}, -4V_{dc}, -5V_{dc}, -6V_{dc}, -7V_{dc}, -8V_{dc}, -9V_{dc})$. The load phase voltages V_{an}, V_{bn} and V_{cn} can be calculated as in (2):

$$\begin{bmatrix} v_{an} \\ v_{bn} \\ v_{cn} \end{bmatrix} = \begin{bmatrix} 2 & -1 & -1 \\ -1 & 2 & -1 \\ -1 & 2 & -1 \end{bmatrix} \tag{2}$$

As the reference voltage increases modulation index (MI), the available levels increases. For 100% MI, the number of available levels is 9, therefore the available levels (N) can be calculated as follows:

$$N = \begin{cases} 9 & MI > 0.75 \\ 7 & 0.75 \geq MI > 0.5 \\ 5 & 0.5 \geq MI > 0.25 \\ 3 & MI < 0.25 \end{cases} \tag{3}$$

The operation of this inverter has been simulated for different values of MI assuming that the main inverter DC voltage is 150V and the auxiliary dc voltage is 50V, results have been tabulated in table II. it can be concluded that for MI around 0.9, the auxiliary inverter contributes with a very small value of load power and the load power is mainly taken from the main inverter. This means that if the operation of the MLI has been fixed at MI around 0.9, the rating of the HFT will be very small which decreases drastically its cost. Therefore the control of the load voltage is executed by fixing the dc inverter voltage.

Fig. 2 shows the HFT that connects the main inverter unit with the auxiliary inverter unit. It composed of HFT with a two switches operate in a complementary mode of operation to supply a switch dc voltage required by the transformer. The transform is a step down with 3/1 turns ratio which is suitable for this specific application and MLI. The main task of this HFT is to generate the dc source of the auxiliary inverter unit from the main transformer unit dc source. By this method, an inherit voltage balancing between the main and auxiliary inverter units is obtained which is very important. This balancing will result in simplifying the control system. Using HFT will decrease the isolated dc sources by half for this MLI. In another way, each

HFT is used to replace a PV module which will also decrease the cost of the whole system.

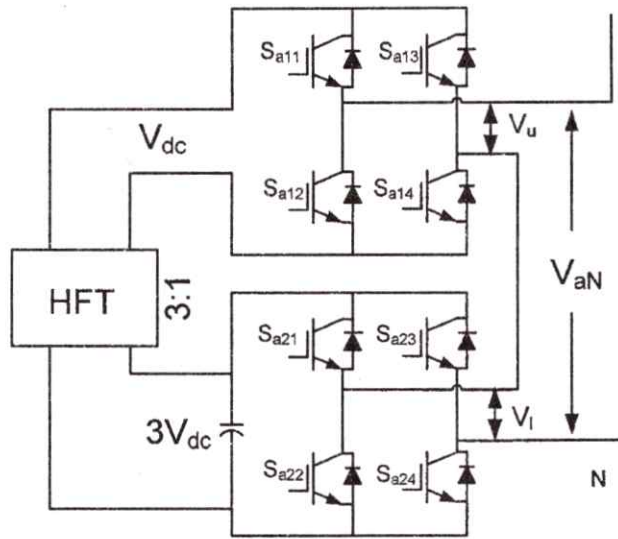


Fig. 1. The conventional 9 level MLI with maximum output voltage resolution

Table I. Simple Switching Description of the Proposed Model

Voltage level (V_{aN})	Sa1	Sa	Sa	Sa	Sa	Sa	Sa2	Sa2
	1	12	13	14	21	22	3	4
$4V_s$	1	0	0	1	1	0	0	1
$3V_s$	1	0	1	0	1	0	0	1
$2V_s$	0	1	1	0	1	0	0	1
$1V_s$	1	0	0	1	0	1	1	0
$0V_s$	0	1	1	0	0	1	1	0
$-V_s$	0	1	1	0	1	0	1	0
$-2V_s$	1	0	0	1	0	1	1	0
$-3V_s$	1	0	1	0	0	1	1	0
$-4V_s$	0	1	1	0	0	1	1	0

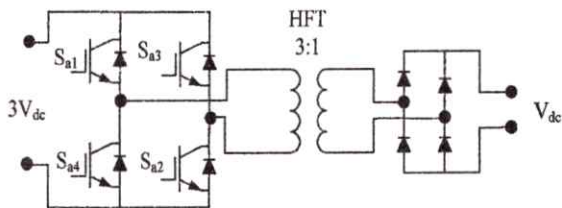


Fig. 2. The upper MLI cell voltage is generated from the lower MLI cell

Table II Results of the MLI with Wide Range of MI

MI	Number of output voltage level	Ratio of contribution of Aux and Main cells: %Aux/Main cells
----	--------------------------------	--

0.9	9	13.9
0.85	9	8.0
0.8	9	7.5
0.75	7	13.5

The dc source of the main inverter unit is generated from the PV module as shown in Fig. 3. It consists of PV module which is the main unregulated dc source, dc-dc converter accompany with maximum power point tracking control required for catching the maximum available power from the PV module, and a storage battery system with a bidirectional dc-dc converter for regulating the dc source at specified voltage value. To get the maximum power from the PV module, the conventional perturb and observe (P&O) [10] – [12] has been adopted in this work. A PV module of BP485 has been chosen with nominal values given in table III. The bidirectional control of the battery energy storage system (BESS) is carried out based on the modified hysteresis control [13] – [14] shown in Figs. 4 and 5.

Table III. PV module BP485 specifications

Rated Power (P_{max})	85W
Voltage at P_{max} (V_{mp})	17.4V
Current at P_{max} (I_{mp})	4.9A
Short circuit current (I_{sc})	5.48A
Open circuit voltage (V_{oc})	22V

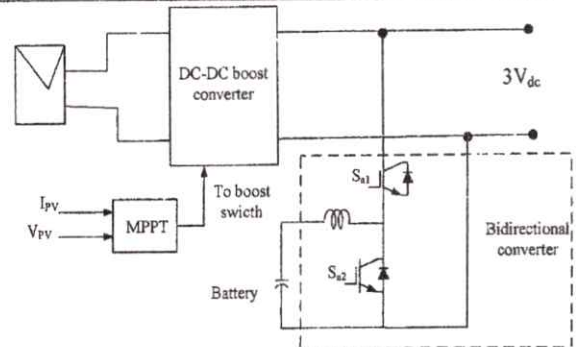


Fig. 3. The lower MLI cell dc voltage source component

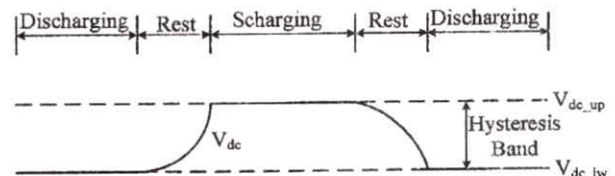


Fig. 4. Modified hysteresis-control strategy

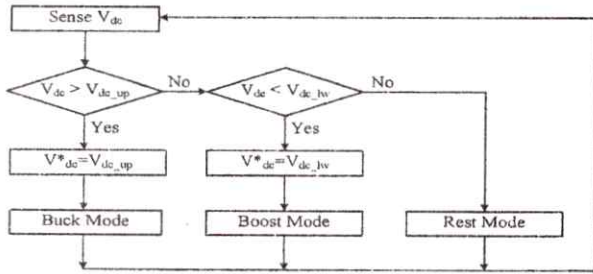


Fig. 5. Battery-mode control block (BESS /modified hysteresis)

3. Results and Discussions

Fig. 6 shows the integration of the above description of the system for single arm (phase). The proposed system has been simulated using MATLAB/SIMULINK[®] to verify the performance of the proposed control. A nonlinear load of three phase full bridge rectifier loaded with a RL load has been chosen with 100Ω resistance and 20 mH inductance.

The dynamic response has been verified due to a sudden change in the load voltage. A sudden change has been taken place by bubbling the load after 0.2 seconds of simulation starting. An ideal electronic switches and diodes have been assumed for simulation.

Fig. 7 shows the simulation results of the battery charger model shown in Figs. 4 and 5. This is for single cell battery of 24 V and 80% rating values of voltage and state of charge (SOC). At 0.2 second the step change shows the change in the battery state from discharging to charging modes where its current changes its polarity from positive into negative sign. Fig. 8 shows the simulations results of on module of the PV model and its ratings are provided in table III. It gives approximately 90W, 20V and 5A of PV values which are very close to the PV maximum power rating provided by its data sheet.

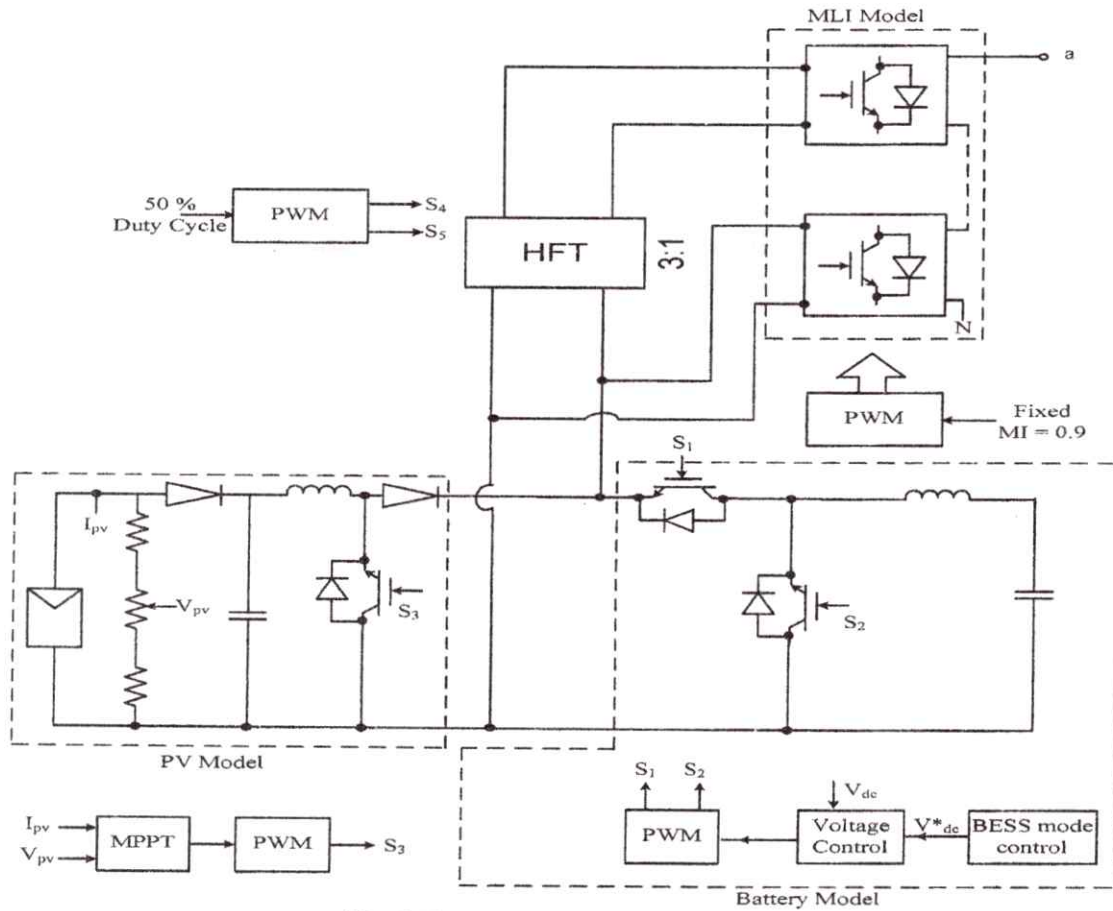


Fig. 6. The proposed multi-level inverter system

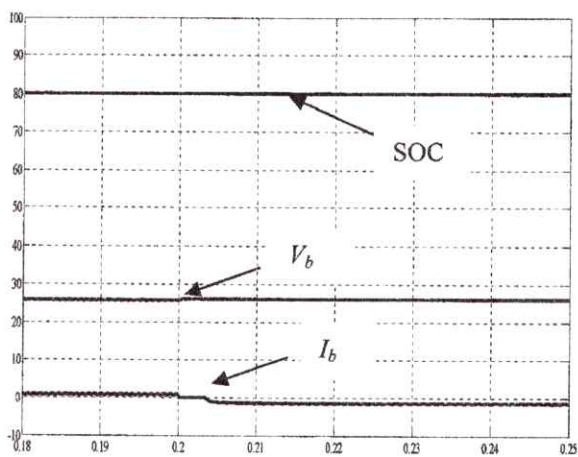


Fig. 7. Battery voltage, current and state of charge for single battery of the storage system

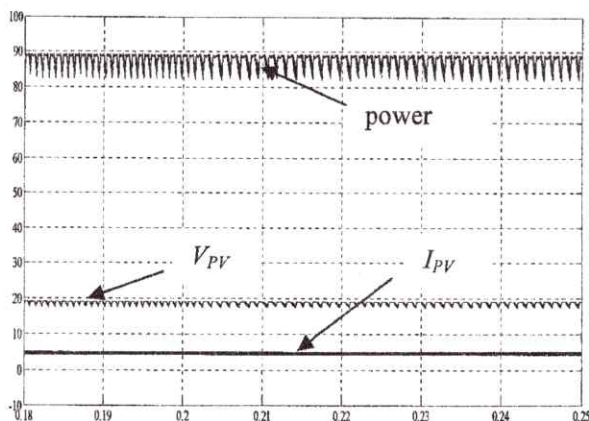


Fig. 8. PV Voltage, current and power at maximum power point for single PV module.

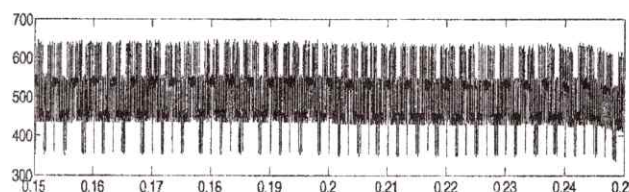
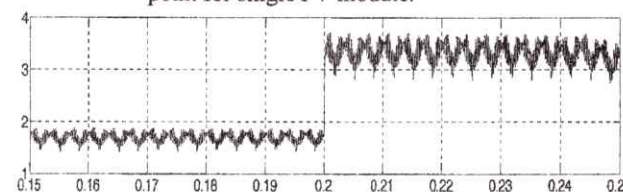


Fig. 9. Load current and load voltage with load step at 0.2 s.

Fig. 9 from top to bottom represents the load current and voltage, respectively. It illustrates that the change in the load current at 0.2 s due to sudden decrease in the load impedance is almost one half of its initial value. The average value of the load current

changed from about 1.8A to 3.6A. In the other hand, the load voltage is almost constant with average value of 530 V and this attributes to the voltage control employed on the dc bus of the ML inverter.

Fig. 10 shows the MLI line currents. It illustrates that line currents increased due to the sudden decreased in the load impedance to about twice of its value after 0.2s. Fig. 11 gives the MLI three phase line-to-line voltages. Since the operation of the MLI is done at constant MI besides the dc bus voltages is kept constant using voltage control, therefore these voltages are kept constant under the dynamic change of the load.

Figs. 12 and 13 show the contribution of the main, auxiliary inverters voltages and currents respectively. Fig. 12 shows the voltages of the auxiliary and main voltages. It indicates that the auxiliary voltages have more switching compared to the main inverter. The main inverter voltages is nearly has load frequency switching. Besides the relative values between the auxiliary inverter voltage and main inverter voltage is 1/3 which comes from the HFT. On the other hand Fig. 13 shows the current contribution of the auxiliary and main inverters. Two observations can be done; 1) the first, the auxiliary inverter current is more switched than the main inverter current; 2) the second, the main inverter current is unidirectional while the auxiliary inverter current is bidirectional. Due to that the average values will follow the design given in table II. This indicates that load is actually supplied from the main inverter. Therefore this will be reflected on the size of the HFT to be very small which is a main task in this work.

Fig. 15 shows the dc bus voltage of the main and auxiliary inverters. The main inverter dc bus is about 270 V and the auxiliary inverter dc bus is about 90 V. the voltage control done the battery banks can guarantee to keep these dc bus voltages at certain specific constant value without change with load changing.

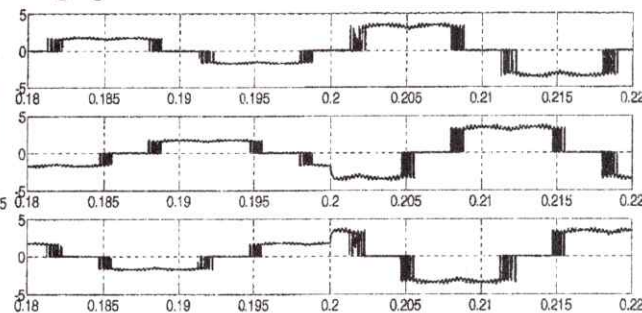


Fig. 10 MLI line currents with load step at 0.2 s.

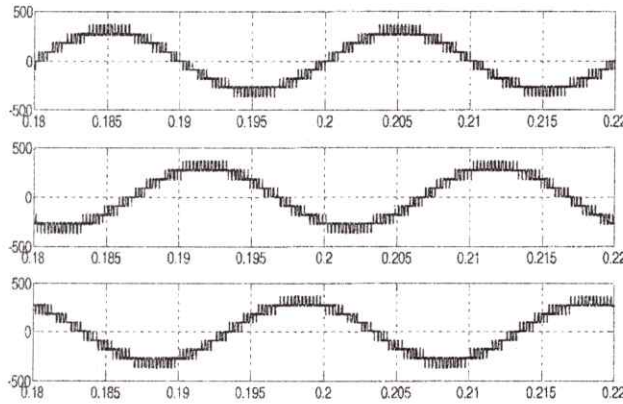


Fig. 11 MLI line-to-line output voltages with load step at 0.2 s.

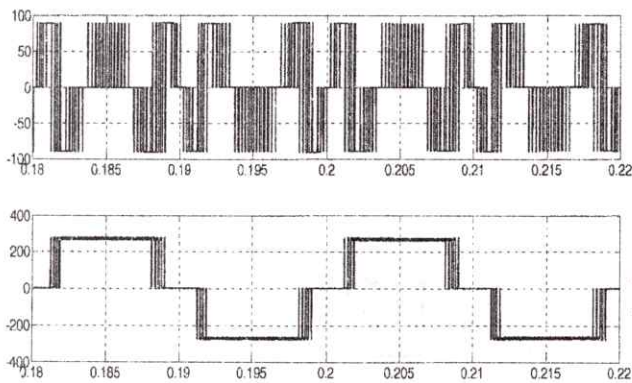


Fig. 12 MLI upper and lower cell voltages.

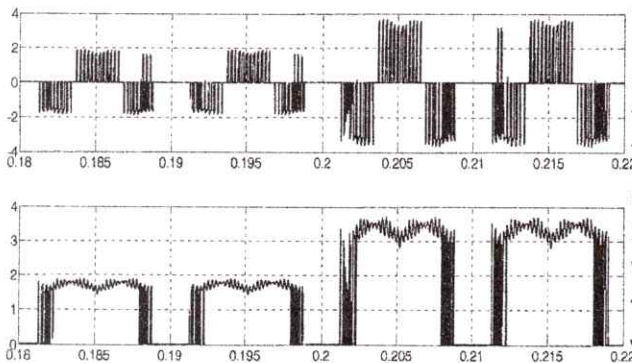


Fig. 13 upper and lower MLI cells currents.

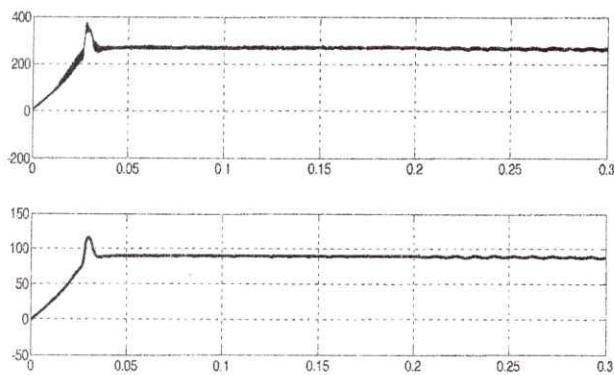


Fig. 14 Lower and upper MLI DC input voltages.

8. Conclusions

This paper presented simulation, analysis and the operation of MLI inverter for standalone PV system applications. The main advantages of the proposed topology are; 1) it has lower number of isolated dc bus voltages, 2) the dc bus voltages of the main and auxiliary inverters are naturally balanced due to using the HFT. In this system a HFT is used per phase to generate the dc bus voltage of the auxiliary inverter from the dc bus of the main inverters. A fixed and optimum MI is chosen to reduce drastically the HFT which is very important in reducing the overall system size. The dynamic performance of the system is tested due to a sudden change in the load voltage. A voltage control technique is employed to keep the dc bus voltage constant where a PV accompany with a BESS is used for this task. Simulation results have been provided for system verification.

References

1. Soeren Baekhoej Kjaer, John K. Pedersen, and Frede Blaabjerg, "A Review of Single-Phase Grid-Connected Inverters for Photovoltaic Modules" IEEE Transactions on Industry Applications, Vol. 41, No. 5, September/October, 2005, pp: 1292 – 1306.
2. Eduardo Román, Ricardo Alonso, Pedro Ibañez, Sabino Elorduizapatarietxe, and Damián Goitia, "Intelligent PV Module for Grid-Connected PV Systems", IEEE Transactions on Industrial Electronics, Vol. 53, No. 4, August 2006, pp: 1066 – 1073.
3. M. N. A. Kadir S. Mekhilef, and H. W. Ping Voltage Vector Control of a Hybrid Three-Stage Eighteen-Level Inverter by Vector Decomposition IET Transaction on Power Electronics, Volume 3, Issue 4, pp.601- 611,
4. Saad Mekhilef, and Mohamad N. Abdul Kadir, "Novel Vector Control Method for Three-Stage Hybrid Cascaded Multilevel Inverter", IEEE Transactions On Industrial Electronics, Vol. 58, No. 4, April 2011.
5. Samir Kouro, Rafael Bernal, Hernán Miranda, César A. Silva, and José Rodríguez, "High-Performance Torque and Flux Control for Multilevel Inverter Fed Induction Motors", IEEE Transactions on

Power Electronics, Vol. 22, No. 6, November 2007, pp: 2116 – 2123.

6. Baruschka, L.; Mertens, A., "Comparison of Cascaded H-Bridge and Modular Multilevel Converters for BESS application", IEEE Energy Conversion Congress and Exposition (ECCE), 2011, pp: 909 – 916.

7. Sepahvand, H.; Jingsheng Liao; Ferdowsi, M., "Investigation on Capacitor Voltage Regulation in Cascaded H-Bridge Multilevel Converters With Fundamental Frequency Switching", IEEE Transactions on Industrial Electronics, Vol.: 58 , Issue: 11, 2011, pp: 5102 – 5111.

8. D. Zhong, B. Ozpineci, L. M. Tolbert, and J. N. Chiasson, "DC-AC Cascaded H-Bridge Multilevel Boost Inverter With No Inductors for Electric/Hybrid Electric Vehicle Applications," Industry Applications, IEEE Transactions on, vol. 45, no. 3, 2009, pp. 963-970.

9. S. Vazquez, J. I. Leon, L. G. Franquelo, J. J. Padilla, and J. M. Carrasco, "DC-Voltage-Ratio Control Strategy for Multilevel Cascaded Converters Fed With a Single DC Source," Industrial Electronics, IEEE Transactions on, vol. 56, no. 7, 2009, pp. 2513-2521.

10. Femia, N.; Petrone, G.; Spagnuolo, G.; Vitelli, M., "Optimization of perturb and observe maximum power point tracking method", IEEE Transactions on Power Electronics, Vol. 20 , Issue: 4, 2005 , pp: 963 – 973.

11. Chee Wei Tan; Green, T.C.; Hernandez-Aramburo, C.A, "Analysis of perturb and observe maximum power point tracking algorithm for photovoltaic applications", IEEE 2nd International Power and Energy Conference, PECon 2008, pp: 237 – 242.

12. Elgendy, M. A.; Zahawi, B.; Atkinson, D. J., "Evaluation of perturb and observe MPPT algorithm implementation techniques", 6th IET International

Conference on Power Electronics, Machines and Drives (PEMD 2012), 2012 , pp: 1 – 6.

13. Seul-Ki Kim, Jin-Hong Jeon, Chang-Hee Cho, Jong-Bo Ahn, and Sae-Hyuk Kwon, "Dynamic Modeling and Control of a Grid-Connected Hybrid Generation System With Versatile Power Transfer", IEEE Transactions on Industrial Electronics, Vol. 55, No. 4, April, 2008, pp: 1677- 1688.

